BBA - Molecular Cell Research 1865 (2018) 863–873

Contents lists available at ScienceDirect

BBA - Molecular Cell Research

journal homepage: www.elsevier.com/locate/bbamcr

Molecular dissection of the membrane aggregation mechanisms induced by monomeric annexin A2

Juan C. López-Rodríguez, Francisco J. Martínez-Carmona, Ignacio Rodríguez-Crespo, M. Antonia Lizarbe, Javier Turnay*

Departamento de Bioquímica y Biología Molecular, Facultad de Ciencias Químicas, Universidad Complutense de Madrid, 28040 Madrid, Spain

ARTICLE INFO

Keywords:
Annexin
Amphipathic helix
Calcium binding
Dimerization
Phospholipid binding
Vesicle aggregation

ABSTRACT

Annexins are a multigene family of proteins involved in aggregation and fusion processes of biological membranes. One of its best-known members is annexin A2 (or p36), capable of binding to acidic phospholipids in a calcium-dependent manner, as occurs with other members of the same family. In its heterotetrameric form, especially with protein S100A10 (p11), annexin A2 has been involved as a determinant factor in innumerable biological processes like tumor development or anticoagulation. However, the subcellular coexistence of different pools of the protein, in which the monomeric form of annexin A2 is growing in functional relevance, is to date poorly described. In this work we present an exhaustive structural and functional characterization of monomeric human annexin A2 by using different recombinant mutants. The important role of the amphipathic N-terminal α-helix in membrane binding and aggregation has been analyzed. We have also studied the potential implication of lateral "antiparallel" protein dimers in membrane aggregation. In contrast to what was previously suggested, formation of these dimers negatively regulate aggregation. We have also confirmed the essential role of three lysine residues located in the convex surface of the molecule in calcium-free and calcium-dependent membrane binding and aggregation. Finally, we propose models for annexin A2-mediated vesicle aggregation mechanisms.

1. Introduction

Annexins (from the Greek *annex*, hold together) are a multigene superfamily of proteins whose primary biological function is cell structure coupling. They are soluble proteins capable of reversible binding to negatively charged membrane phospholipids in a calcium-dependent process [1,2]. Widely described in all organisms, annexins present a conserved C-terminal core formed by the repetition of four (or eight) homologous domains of about 70 amino acids each, formed by five α-helixes (named A-D), four of them forming a superhelix (A, B, D, E). The protein core forms a compact and protease resistant structure differentiating a slightly curved convex region, where type-II calcium and phospholipid binding sites are located, and a concave side where a hypervariable N-terminal domain lies [3,4]. Fig. 1a shows the three-dimensional structure of human annexin A2 where the above-mentioned general structural characteristics of the annexin superfamily can be observed. Protein modifications and their interaction with other cytosolic proteins are mainly regulated by N-terminal dynamics and its accessibility to the solvent [4].

Annexins are mostly related to membrane trafficking, the regulation of membrane-cytoskeleton interactions and microdomain formation [5]. One of the best known members that has been associated with membrane aggregation and raft-microdomain formation in cells has been human annexin A2 (also called p36). Unlike some members of the annexin superfamily, annexin A2 binding to acidic phospholipid vesicles seems to be accomplished not only by a Ca^{2+}-dependent mechanism [6]. Annexin A2 hetero-oligomerization with proteins of S100 family (*e.g.* S100A10, p11) reduces Ca^{2+}-aggregation requirements [7], but there is also strong evidence of *in vitro* bridging processes involving monomeric annexin in the absence of calcium [8]. Lipid-binding capacity of annexin A2 has been proposed to be regulated by the N-terminal segment (residues 1–29) [9]. This region contains not only the S100A10 dimer-binding site, but also sites susceptible of phosphorylation, acetylation and S-glutathionylation, that might regulate calcium sensitivity and lipid binding [10–12]. Ca^{2+}-independent binding of monomeric annexin A2 to membranes has been observed in both model

Abbreviations: BS^3, (*bis*[sulfosuccinimidyl]suberate); LUVs, Large Unilamellar Vesicles; PC, Phosphatidylcholine; PS, phosphatidylserine; TK-hA2, human annexin A2 with residues K^{49}, K^{206} and K^{281} replaced by alanines; TM-hA2, human annexin A2 with residues E^{189}, R^{196} and E^{219} replaced by alanines; WT-hA2, Wild-Type human annexin A2; Δ14-hA2, truncated human annexin A2 lacking the first N-terminal 14 residues

* Corresponding author.
E-mail address: turnay@ucm.es (J. Turnay).

https://doi.org/10.1016/j.bbamcr.2018.03.010
Received 4 December 2017; Received in revised form 13 March 2018; Accepted 14 March 2018
Available online 19 March 2018

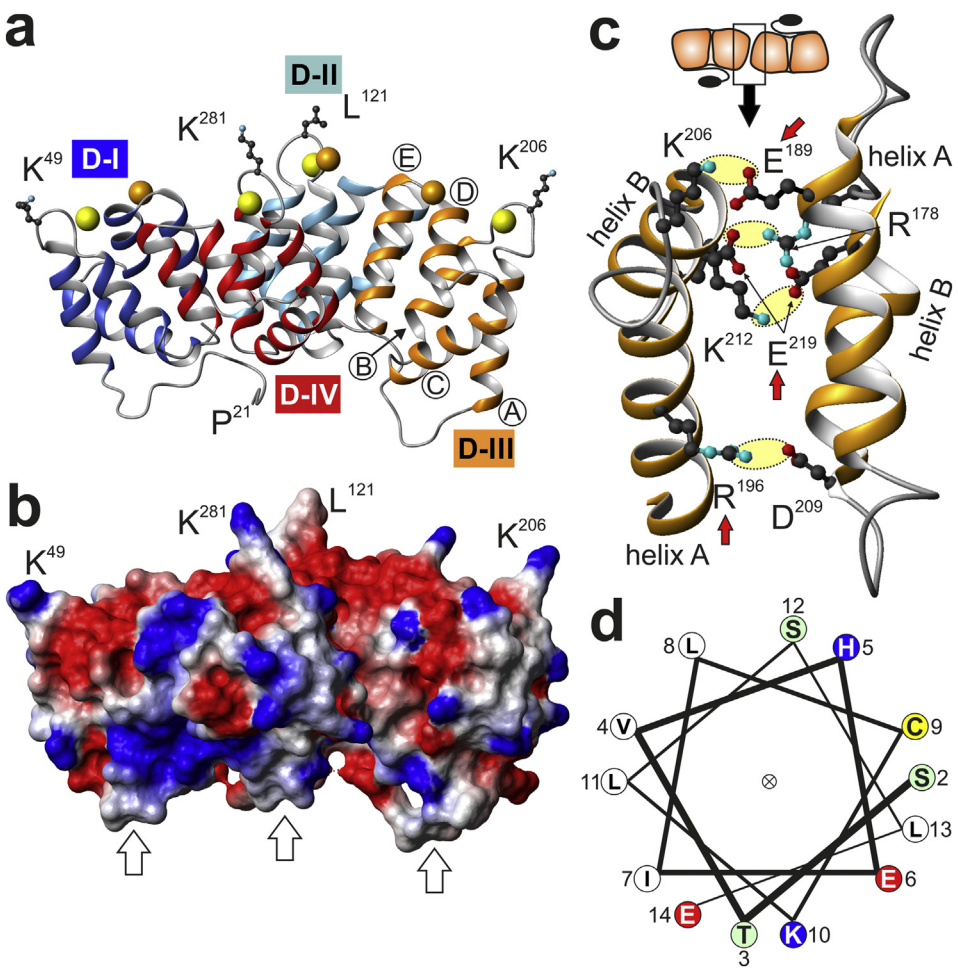

Fig. 1. Three-dimensional structure of full-length annexin A2.
(a) Three-dimensional structure of full-length annexin A2 based on the crystallographic data from PDB ID: 1XJL [31] using MOLMOL [53]. The four domains in the protein core are represented in different colors: I, blue; II, cyan; III, orange; and IV, red. The letters assigned to the α-helices are shown only in Domain III. Calcium ions at the canonical type-II binding sites (or "AB" sites) are represented by yellow spheres; additional calcium ions bound to the so-called "DE" or "B" sites [3] are shown as orange spheres. The side-chains of the three mutated lysine residues located in the AB-loops of domains I, III, and IV, and the leucine residue in domain II are also indicated. **(b)** Surface representation showing positively charged (blue), negatively charged (red) and uncharged regions (white). Empty arrows indicate the uncharged regions in the concave surface that may be involved in dimerization. **(c)** Detail of the dimer interface between two annexin A2 molecules through residues located in domain III of each molecule according to the structure by Rosengarth and Luecke [31]. Mutated residues in TM-hA2 are indicated with a red arrow. **(d)** Helical wheel representation of residues 2 to 14 corresponding to the N-terminal extension of annexin A2.

vesicles and chromaffin granules. This may imply a pH-dependent process likely involving dynamic changes on N-terminal hydrophobicity at acidic pH [13,14], although some details of the process remain misunderstood.

Numerous studies have been focused on the subplasmalemal heterotetrameric complex with S100A10 dimer. However, different pools of monomeric annexin A2 have been described in lung epithelium derived-cells, existing cytosolic, nuclear and endosomal fractions, as well as an additional pool that strongly interacts with membranes in a calcium-independent manner [15]. As occurs with the heterotetramer, monomeric annexin A2 can also induce membrane domain formation by promoting lipid clustering of vesicles composed of phosphatidylserine (PS) and phosphatidylinositol-4,5-bisphosphate in the presence of cholesterol [16,17]. Annexin A2 has been also described as a positive regulator of calcium-dependent plasma membrane resealing in primary human vascular endothelial cells [18]. Monomeric annexin A2 has been recently reported to have immunological functions by inducing murine and human dendritic cell maturation through Toll Like Receptor 2 (TLR2) under oxygen depletion, being the N-terminal 15 amino acids of this annexin necessary and sufficient for TLR2 binding and dendritic cell activation [19]. Moreover, the specific inhibition of monomeric annexin A2 binding to PS -and not in its tetrameric form- prevents from HIV-1 infection in monocyte-derived macrophages [20], in a similar way to that described for the secretory leukocyte protease inhibitor (SLPI) [21]. Annexin A2 is highly expressed in most cancers where it is involved in extracellular plasmin activation, and thus activation of metalloproteinases and degradation of extracellular matrix components essential for metastatic progression [22]. Interestingly, treatment of human colon cancer cell lines with active matrilysin (matrix metalloprotease-7) releases annexin A2 from the membrane by hydrolysis of the peptide bond between Lys^{10} and Leu^{11}; this release significantly enhances binding of tissue-type plasminogen activator to cancer cell surfaces probably *via* the membrane-bound hydrolyzed N-terminal peptide [23] reinforcing the potential role of the N-terminus of annexin A2 in its binding to membranes under specific conditions. In addition, nuclear monomeric annexin A2 has been related with cell proliferation and DNA synthesis regulation [24,25].

In the present work, we have deepened into the structural and functional events involving human annexin A2 interaction with membranes by using lipid model vesicles. Different *Escherichia coli*-expressed mutants were designed and characterized by spectroscopical and functional assays. Our results not only support the key role of the N-terminal region in monomeric annexin A2-mediated aggregation, but also demonstrate the existence of residues that are additionally controlling protein homo-dimerization and the aggregation process.

2. Materials and methods

2.1. Construction of wild-type and mutant human annexin A2 expression vectors

The construct expressing recombinant human annexin A2 was generated by cloning its cDNA between *Bam*HI and *Xho*I restriction sites of the pBH4 vector (kindly provided by Wendell Lim, UCSF) to generate an N-terminal 6xHis-tagged, TEV-cleavable protein. The deletion mutant without residues 1–14 at the N-terminus of annexin A2 (Δ14-hA2 protein) was generated by PCR using the QuickChange method with pBH4.WT-hA2 as template to obtain construct pBH4.Δ14-hA2. Point

mutations were also carried out by the QuickChange method by sequential mutation of single residues to obtain constructs pBH4.TM-hA2 (mutations E189A, R196A & E219A; TM-hA2 protein) and pBH4.TK-hA2 (mutations K49A, K206A & K281A; TK-hA2 protein). Primers used for QuickChange site-directed mutagenesis are shown in Supplementary Fig. 1. These primers also introduced new restriction sites for screening. In addition, all constructs were sequenced in both directions to verify the correct insertion of the point mutations without any additional modifications.

2.2. Protein expression and purification

Recombinant variants of annexin A2 were produced in BL21(DE3) *E. coli* strain and purified by Ni-NTA-agarose chromatography after solubilization in the absence of calcium. All these procedures, as well as the removal of the His-tag, were carried out as previously described by our group [26–29] and is presented in detail under *Supplementary material* (Supplementary Fig. 2).

2.3. Circular dichroism measurements

The far-UV CD spectra were monitored between 200 and 260 nm at 20 °C in a Jasco J-715 spectropolarimeter equipped with a Neslab RTE-111 thermostat using 0.05 or 0.01 cm pathlength thermostatized cuvettes. Near-UV CD spectra were monitored between 250 and 320 nm at 20 °C using 0.5 cm pathlength thermostatized cuvettes. All spectra were averaged at least over six scans and were corrected by subtracting buffer contribution from parallel spectra in the absence of protein; units are expressed as mean residue weighed molar ellipticities ($[\theta]_{MRW}$) in the far-UV, and as molar ellipticities in the near-UV. Melting curves were determined by monitoring ellipticity changes at 208 nm between 20 and 80 °C and increasing temperature at 60 °C/h due to the irreversibility of the denaturation process; melting temperatures *(Tm)* were determined from the maximum of the first derivative of the smoothened melting curves, as previously described [26–28]. The effect calcium binding on the far-UV CD spectra and melting temperatures was analyzed employing protein samples with increasing $CaCl_2$ concentrations. Control samples contained 1 mM EGTA or equivalent ionic strength with $MgCl_2$. Secondary structure prediction from the far-UV CD spectra was performed using the convex constraint algorithm (CCA) as described [30].

2.4. Fluorescence emission spectroscopy

Fluorescence emission spectra (300–400 nm) were recorded in an SLM Aminco 8000C spectrofluorimeter at 20 °C. Trp^{213} emission was measured using an excitation wavelength of 295 nm in a 0.4 cm excitation pathlength and 1.0 cm emission pathlength cuvette. Rayleigh scattering at 90° was obtained from the maximum at 295 nm of spectra recorded at this excitation wavelength. Spectra were recorded either in the absence of calcium (1 mM EGTA) or after the addition of increasing volumes of a concentrated buffered $CaCl_2$ solution up to 75 mM (controls in the presence of $MgCl_2$ were also studied). Acrylamide quenching of Trp^{213} fluorescence was analyzed by recording emission spectra (295 nm excitation wavelength) at increasing acrylamide concentration, and taking into account the effect of dilution as previously described [26–28]. Care was taken to avoid the inner filter effect and that solutions presented always UV absorption below 0.04 at 295 nm. The quenching constants (K_{SV}) were calculated from the Stern-Volmer plots of F_0/F at the emission maximum against acrylamide concentration, according to the equation $F_0/F = 1 + K_{SV}[Q]$, where F_0 is the fluorescence intensity at zero quencher concentration and F the intensity at a given quencher concentration ($[Q]$).

2.5. Binding to phospholipids and vesicle aggregation assays

Large unilamellar vesicles (LUVs) of phosphatidylserine (PS) (Avanti Polar Lipids, Alabaster, AL, U.S.A.) or phosphatidylcholine (PC) were obtained by film hydration in 10 mM Hepes, pH 7.8, containing 0.1 M NaCl, followed by extrusion through polycarbonate filters of 400 nm pore diameter (Lipex Biomembranes, Vancouver, Canada). 100 nm pore LUVs were prepared from previously obtained 400 nm fresh vesicles by further extrusion through filters of the corresponding pore diameter.

The binding of the purified recombinant proteins to 400 nm vesicles was carried out at a constant lipid:protein molar ratio (800:1) with variable calcium and NaCl concentrations in 10 mM Hepes, pH 7.8, for 15 min at room temperature. The final volume (100 µl) was ultracentrifuged at 150,000 *g* at 4 °C for 1 h (Optima Max-XP ultracentrifuge with TLA 120.1 rotor; Beckman-Coulter, Brea, CA). After the separation of supernatant and pellet, equivalent volumes were analyzed by SDS-PAGE under reducing conditions and Coomassie blue staining or Western blot. Vesicle-free controls showed very little or null sedimentation of protein under these experimental conditions. Gels were analyzed in a Gel Doc XR system from Bio-Rad (Alcobendas, Spain) and a densitometric analysis was performed by using the QuantityOne v4.6.9 software. The percentage of bound protein was determined from at least three independent experiments in which all conditions were analyzed in the same gel.

Aggregation assays were carried out by recording absorption at 320 nm immediately after the addition of the lipids to a solution containing different concentrations of protein, NaCl (0.1, 0.3 or 0.5 M) and in the absence (5 mM EGTA) or presence of 100 µM $CaCl_2$. Absorption was registered in a thermostatically controlled cuvette for at least 10 min at 25 °C. No variation in the absorbance at 320 nm was observed in PS vesicles (with or without 100 µM $CaCl_2$) in the absence of protein. These absorbance baseline values were subtracted from the corresponding aggregation curves. Apparent initial aggregation velocity (V_0 app.) was determined from the non-linear regression to a hyperbola of the aggregation curve up to only 1 min.

2.6. Protein crosslinking in the presence of PS-vesicles

Protein crosslinking in the absence or presence of 400 nm PS-vesicles (1000:1 lipid:protein molar ratios; 2 µM protein) was carried out after 15 min of interaction in the absence (5 mM EGTA) or presence of 100 µM $CaCl_2$. Additionally, different concentrations of NaCl (0.1, 0.3 and 0.5 M) were tested. Whole volume was further incubated with BS^3 cross-linker (1 mM final concentration; Pierce, Rockford, IL, U.S.A.) for 30 min at room temperature. This reaction was stopped by addition of Tris, pH 7.4 (100 mM final concentration) for 15 min at room temperature. Samples without vesicles were directly prepared for SDS-PAGE; samples with PS-vesicles were ultracentrifuged at 150,000 *g* at 4 °C for 1 h and pellets were resuspended into the same volume as those without vesicles directly in loading buffer. All samples were analyzed by Western blot using a monoclonal antibody directed against human annexin A2 (BD Biosciences).

2.7. Statistical analysis

The normal distribution of data was determined by the Shapiro-Wilk test and the homogeneity of variance by the Brown-Forsythe test. Two-way ANOVA analyses and Student's *t*-tests (two-tailed) were carried out using SigmaPlot v13 (Systat Software, Erkrath, Germany) and $p < 0.05$ was taken as the minimal level of statistical significance.

3. Results and discussion

3.1. Cloning, expression and purification of recombinant annexin A2 and mutants

In 2004, *Rosengarth and Luecke* published the three-dimensional structure of full-length annexin A2 in the presence of calcium (PDB ID: 1XJL; Figs. 1a & 1b) and a N-terminally truncated structure in the absence of calcium (PDB ID: 1W7B) [31]. Both structures were essentially similar but, interestingly, in the presence of calcium the protein formed what they called an "upside-down" (or "antiparallel") dimer. In this crystal, one monomer has the convex surface on the same side as the concave surface of the other one. This arrangement resulted in a dimer with calcium binding sites on both sides (Fig. 1c). The interaction between monomers took place side by side through the establishment of four salt bridges between residues located in domain III of both proteins: Arg A196-Asp B209, Lys A206-Glu B189, Glu A219-Arg B178 and Lys A212-Glu B219. In view of this arrangement the authors proposed that, theoretically, this dimer could bind two membranes at the same time inducing aggregation in a similar way as reported for bovine annexin A6, whose two lobes (4 domains each) were reported to interact in an "antiparallel" arrangement with phosphatidylserine monolayers [32]. In any case, the mechanism by which annexin A2 induces membrane aggregation is not clear yet. For this reason, we decided to check whether this hypothesis was accurate by inducing point mutations affecting residues involved in the establishment of the reported salt-bridges (Fig. 1c); Glu^{189}, Arg^{196} and Glu^{219} were replaced by alanine residues blocking in this way the formation of the four bridges (Triple Mutant; TM-hA2).

It is also worth mentioning that several studies point out the important role that the first 14 residues of the N-terminal segment of annexin A2 may have in binding and aggregation of biological membranes. We have run prediction algorithms, as "Helixator" (TCDB; http://www.tcdb.org) or "Heliquest" [33], and both predict the potential arrangement into an amphipathic α-helix (Fig. 1d), as detected in water/TFE mixtures [34] and when complexed with S100A10 or S100A4 protein dimers [35,36]. Thus, in the set of mutations directed to dissect the mechanism by which annexin A2 induces membrane aggregation, we have obtained a deletion mutant lacking the first 14 amino acids (Δ14-hA2).

Finally, the convex face of annexin A2 molecule is mainly negatively charged (Fig. 1b) but exhibits some protruding positively charged residues such as Lys^{49}, Lys^{206} and Lys^{281}, which are located in the loops between helices A and B of domains I, III and IV, respectively. These residues may be involved in establishing electrostatic bridges with negatively charged phospholipids. Considering this, we have also obtained an annexin A2 mutant lacking these three protruding lysine residues (replaced by alanines; TK-hA2; see Figs. 1a & 1b).

Site directed mutagenesis and deletion mutants were obtained by the QuickChange protocol, as described in *Supplementary material*. All constructs were cloned into the expression vector pBH4 and were transformed into BL21(DE3) *E. coli* strain. Production, purification and His-tag removal of the recombinant proteins is described in detail in *Supplementary material* (Supplementary Fig. 2).

3.2. Spectroscopical characterization of recombinant proteins

Far-UV circular dichroism reveals a proper folding of all proteins (Fig. 2a). According to CCA algorithm [30], all of them present a high α-helical content ranging from 61.7% in WT-hA2 to around 74% in the mutant with the deletion of the 14 first residues (Δ14-hA2). These results are in quite good agreement with the reported three-dimensional structure of annexin A2, showing the crystal a secondary structure almost identical to that predicted for WT-hA2 in solution. The removal of the amphipathic N-terminal α-helix increases α-helical content instead of decreasing it. Thus, it is possible that in the absence of membranes or S100A10 protein, this helix is not formed. In any case, we have previously reported that long N-terminal extensions normally induce a reduction in the α-helical content of the protein core, as occurs with annexin A11 [27] or with the long and short isoforms of annexin A13 [26,28].

Thermal stability was analyzed by recording the molar ellipticity at 208 nm as a function of temperature, as the main structural component of annexin A2 is α-helix. All melting curves show a highly cooperative transition disregarding the calcium concentration used. Unfolding is always irreversible, as cooling of the denatured preparations does not recover the molar ellipticity values (not shown). Thermal stability in the absence of calcium is slightly higher for the truncated form (56.7 ± 0.4 °C) compared to WT-A2 (55.1 ± 0.3 °C) (Fig. 2b & c) in a similar pattern to what occurs with truncated annexin A13b or when the stability of its short isoform (A13a) is compared with the long one (A13b) [26,28]. Whereas the replacement of protuberant lysine residues for alanines does not modify the thermal stability of the protein (TK-hA2 protein; 55.6 ± 0.4 °C), the disappearance of the salt bridges between domains III of annexin A2 molecules induces a significant reduction in the melting temperature (TM-hA2; 50.6 ± 0.6 °C), 4.5 °C lower than wild-type annexin A2. According to all the other mutants, the formation of the lateral dimers could be taking place without calcium, thus stabilizing annexin A2 soluble structures.

We wanted to analyze the effect of calcium binding on the structure and stability of annexin A2 as binding of annexins to membranes is normally calcium-dependent and involves small structural rearrangements that can affect both the protein core and the N-terminal extension. The analysis of the effect of calcium binding in the absence of membranes requires the use of millimolar concentrations of $CaCl_2$, as it is well known that the affinity of annexins for this cation is around three orders of magnitude lower under these conditions [29,37]. For this reason, we used a calcium concentration far away from physiological levels (1.5 mM extracellular; around 100 nM intracellular but with transient spikes up to 1–10 μM; 100–400 μM Golgi and endoplasmatic reticulum) [26,38–40] but necessary to reproduce calcium saturation in the absence of membranes. Far-UV CD spectra does not change significatively upon calcium saturation (up to 95 mM $CaCl_2$; data not shown) but all the recombinant proteins show higher thermal stability with an increase of 12–13 °C in their melting temperatures, calcium specific and non-reproducible with $MgCl_2$ (Fig. 2b & c). Half-maximal effect is achieved at 8.4 mM $CaCl_2$ in WT-hA2 but it is lower for the mutated forms, ranging from 2.5 mM for TM-hA2 to around 5 mM for Δ14-hA2.

In order to analyze whether the tertiary structure surrounding the only Trp residue in annexin A2 (and mutated variants) is modified by calcium binding, we first registered fluorescence emission spectra with an excitation wavelength of 295 nm (Fig. 3a) in the presence of different calcium concentrations, as the position of the emission maximum gives information regarding the exposition degree of the Trp^{213} residue. In the absence of calcium, WT-hA2 shows a maximum at 329 nm and a slight blue shift towards 324 nm with a decrease in the quantum yield (Fig. 3b) that presents a mid-point at 250 μM $CaCl_2$. Saturation of the effect of calcium binding in the environment of Trp^{213} is achieved at a calcium concentration much lower than that required for changes in thermal stability. Taking into account that this residue is located in helix IIIB, one could speculate that Trp environment is only changed when calcium is bound to the high affinity sites (type II calcium binding sites in the loops between helices A and B in each domain). On the other hand, structural stability is further strengthened by calcium binding to additional sites, as those at the DE loops or at helix B, as reported in the calcium-bound crystal structures of annexin A2 and in other annexins [3,31,41].

No significant differences were detected in the fluorescence emission spectra of annexin A2 variants compared to WT-hA2 as well as in the behavior upon calcium binding (data not shown). In all cases, the position of the maximum suggests that Trp^{213} may be somewhat buried,

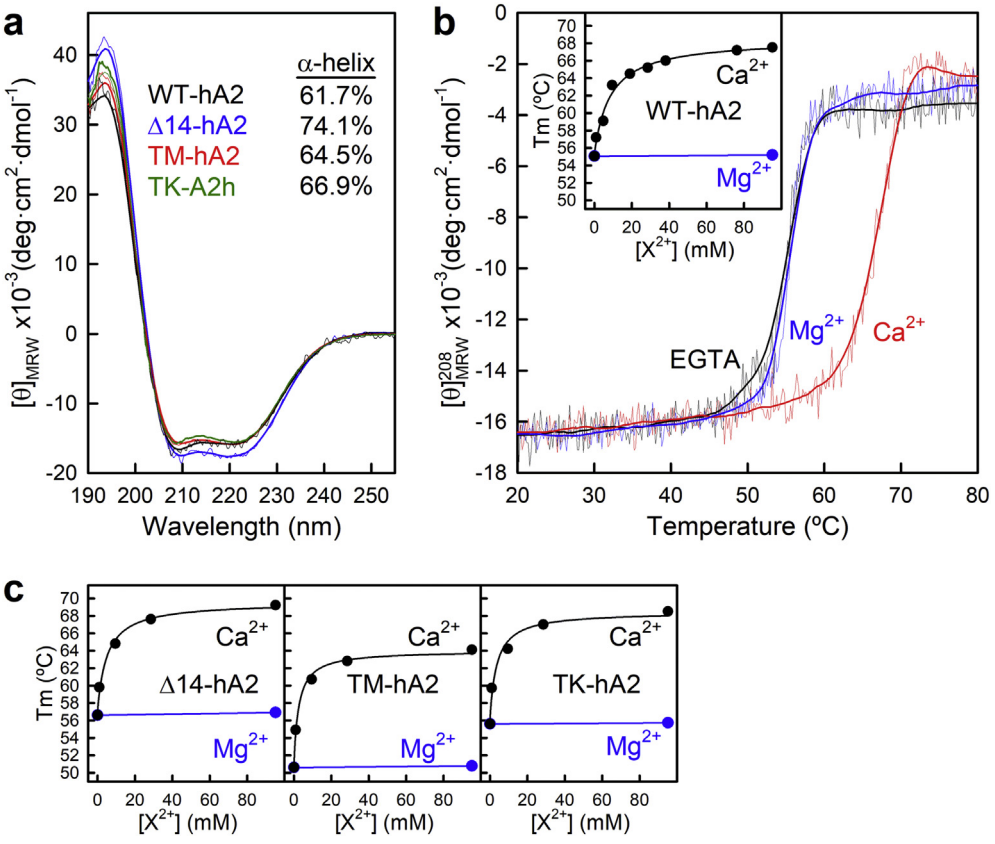

Fig. 2. Far-UV circular dichroism spectra of annexin A2 and mutants.
(a) Far-UV CD spectra of wild-type annexin A2 and the different mutants used in the study were registered in 10 mM Hepes, pH 7.8, 0.1 M NaCl at 20 °C. Each spectrum is the average of six scans; smoothened spectra are also shown. The inset indicates the percentage of α-helix of each protein according to CCA algorithm. **(b)** Influence of calcium binding on the thermal stability of WT-hA2. The figure shows only representative melting curves of in the absence (1 mM EGTA) and in the presence of 95 mM $CaCl_2$ in 10 mM Hepes, pH 7.8, and 0.1 M NaCl. The inset shows the melting temperatures (Tm) at increasing calcium concentrations; they were determined from the inflexion point of the smoothened melting curves (position of the maximum of the first derivative) using the Standard Analysis software from Jasco, and data represent mean values of at least two independent determinations at each $CaCl_2$ concentration. Blue symbols show the effect of 95 mM $MgCl_2$. **(c)** Dependence of the T_m with calcium (black) and magnesium concentration (blue) for the mutant variants of annexin A2.

being even more protected with calcium. This is confirmed by dynamic fluorescence emission quenching experiments using acrylamide, which presents low accessibility to buried residues. Stern-Volmer plots (F_0/F) in Fig. 3c correspond to fluorescence emission data of WT-hA2 in the absence of calcium (1 mM EGTA; 329 nm) and after saturation with calcium (75 mM $CaCl_2$; 324 nm); quenching constants (K_{SV}) under both experimental conditions are quite low, and correspond to a buried Trp residue (1.89 M^{-1} and 0.84 M^{-1} in the absence or presence of calcium, whereas an exposed Trp residues yields values around 12–15 M^{-1}) [42]. Quenching constants for the different annexin A2 mutants (Fig. 3c) are quite similar to those observed for the wild-type, which supports the correct folding of these annexin A2 variants. The decrease in fluorescence emission upon calcium saturation, that is observed on all the analyzed recombinant proteins, could be explained if Trp^{213} establishes hydrogen bonds between the nitrogen atom of the indole ring and the carbonyl oxygen of Leu^{198} which lies nearby in helix IIIA according to the crystal structure of calcium-bound annexin A2 [31].

Near-UV circular dichroism confirms that Trp^{213} lies within the hydrophobic protein core with low conformational freedom as a clear ellipticity minimum appears in all recombinant proteins at 280 nm (Fig. 3d). Moreover, the minimum reaches higher negative values in the truncated form of annexin A2. This can indicate that a more compact structure is present after shortening of the N-terminal region in agreement with the increase in structural stability detected in the analysis of the melting curves.

In summary, the spectroscopical characterization of recombinant wild-type annexin A2 and the different mutants confirm the correct folding of all the protein analyzed, which is essential for the correct analysis and comparison of their behavior regarding binding to membranes and ability to induce vesicle aggregation.

3.3. Phospholipid binding

The interaction of annexin A2 with phospholipid vesicles was studied by ultracentrifugation after incubation of the wild-type protein or the different mutants with an excess of large unilamellar vesicles (LUVs 400 nm in diameter) in the absence (1 mM EGTA) or presence of $CaCl_2$. Different NaCl concentrations were also used to increase ionic strength to debilitate potential salt bridges or increase non-electrostatic interactions (Fig. 4). Sedimented material and supernatants were further analyzed by SDS-PAGE followed by Coomasie blue staining or Western blot and densitometric analysis. As observed in Fig. 4a, protein sedimentation is minimal in the absence of phospholipid vesicles (w/o PS lanes) and no significant variations were observed in the presence or absence of calcium or at increasing NaCl concentrations (data not shown). In any case, these control values were always subtracted from the corresponding densitometric analysis of sedimented proteins in the presence of LUVs.

We first analyzed binding of WT-hA2 to phosphatidylcholine (PC) and phosphatidylserine (PS) LUVs at different calcium concentrations and 0.1 M NaCl (Table 1). No significant binding to PC LUVs was observed whereas binding to PS was close to 50% in the absence of calcium (Table 1; Fig. 4b; 1 mM EGTA) and significantly higher with calcium reaching 100% at 100 μM. Unlike most annexins, annexin A2 is able to bind to vesicles in the absence of calcium; thus, the molecule must present unique regions or residues that allow this calcium-independent binding. In order to analyze this possibility, we have studied the binding of the different mutant variants of annexin A2 to LUVs as model system.

Removal of the N-terminal first 14 residues (Δ14-hA2) brought similar results to those observed in WT-hA2: almost no binding to PC LUVs, 27% binding to PS in the absence of calcium, and very similar binding percentages to PS in the presence of calcium. The decrease in calcium-independent binding to PS (around 23%) strongly suggests that annexin A2 can bind to membranes not only through the canonical type II calcium-binding sites, but also through the amphipathic N-terminal extension, as was also previously suggested by Tsunezumi et al. [23] in human colon cancer cells. However, there must be an additional

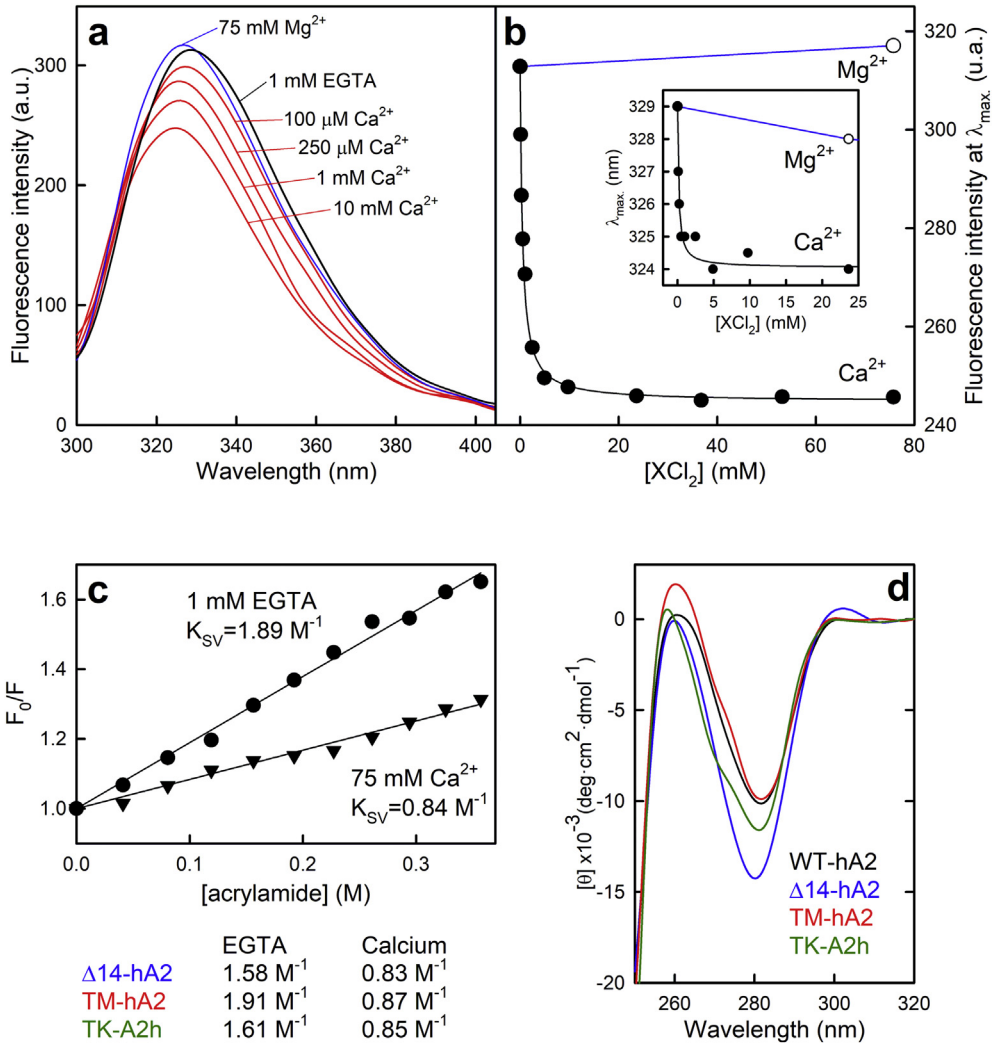

	EGTA	Calcium
Δ14-hA2	1.58 M^{-1}	0.83 M^{-1}
TM-hA2	1.91 M^{-1}	0.87 M^{-1}
TK-A2h	1.61 M^{-1}	0.85 M^{-1}

Fig. 3. Characterization of the unique tryptophan residue of annexin A2 by fluorescence spectroscopy and near-UV circular dichroism. **(a)** Emission spectra at 295 nm excitation wavelength in the absence of calcium (1 mM EGTA) or at increasing $CaCl_2$ (red) or $MgCl_2$ (blue) concentration were registered at 20 °C using a protein concentration of 5 μM. Only spectra of WT-hA2 at representative calcium or magnesium concentrations are shown. Fluorescence is expressed in arbitrary units (a.u.). **(b)** Variation in the fluorescence intensity of Trp^{213} in WT-hA2 at the position of the emission maximum (inset) with calcium concentration (open circle, $MgCl_2$ instead of $CaCl_2$). **(c)** Fluorescence emission (λ_{ex} = 295 nm) at 20 °C of Trp^{213} in wild-type and mutant annexin A2 variants (0.2 mg/ml) was quenched by sequential addition of a concentrated acrylamide stock solution up to 360 mM both in the absence of calcium (1 mM EGTA) and in the presence of 75 mM $CaCl_2$. Fluorescence intensity at 329 nm (absence of calcium; filled circles) or at 324 nm (75 mM $CaCl_2$; open circles) was determined and the data were plotted against acrylamide concentration according to the Stern-Volmer equation (plot shows results for WT-hA2). Stern-Volmer constants (K_{SV}) for all the annexin A2 variants are shown. **(d)** Near-UV CD spectra of WT-hA2 and the different mutants were registered in 10 mM Hepes, pH 7.8, 0.1 M NaCl at 20 °C using a 0.5 cm pathlength cuvette an a protein concentration around 25 μM. Each spectrum is the average of six scans; smoothened spectra are shown.

calcium-independent binding mechanism, as there is still close to 30% binding of Δ14-hA2 under these conditions.

To gain further information on the different mechanisms by which annexin A2 can bind to membranes, we studied the interaction of additional mutant variants to PS LUVs in the absence or presence of 100 μM $CaCl_2$, and at different NaCl concentrations (Fig. 4).

In the absence of calcium, an increase in the ionic strength induces an almost complete blockage of WT-hA2 binding to PS, which puts forward the relevance of ionic interactions between annexin A2 and negatively charged phospholipids. Mutation of residues involved in the "antiparallel" lateral dimerization of annexin A2 (TM-hA2) does not induce a significant variation in binding, but its interaction with PS is less sensitive to the increase in NaCl concentration. On the contrary, mutation of the protruding Lys residues on the convex side of annexin A2 (TK-hA2) reduces binding to only 12.5% and disappears at increasing ionic strength. These results demonstrate experimentally for the first time the involvement of these residues in annexin A2 binding to membranes, as was hypothesized previously by Zibouche et al. [14]. Moreover, a recent publication by Hakobyan et al. [43] carrying out molecular dynamics simulations of the interaction of human annexin A2 with negatively charged membranes has identified *in silico* several Lys residues that may be essential for the calcium-independent binding

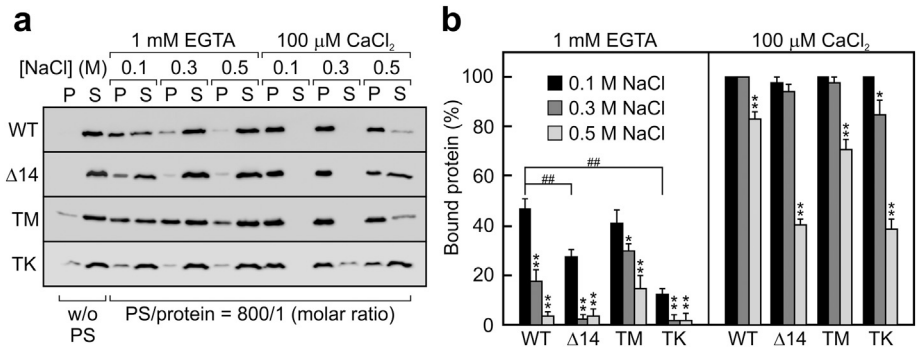

Fig. 4. Binding of annexin A2 variants to phosphatidylserine vesicles. **(a)** The binding of recombinant annexin A2 variants to 400 nm PS unilamellar liposomes was performed by ultracentrifugation in the absence of calcium (1 mM EGTA) or in the presence of 100 μM $CaCl_2$ with a lipid/protein molar ratio of 800/1 and at three different NaCl concentrations. Protein in the supernatants (S) and in the pellets (P) was analyzed by SDS-PAGE followed by Coomassie blue staining; representative gels are given. **(b)** Densitometric analysis corresponding to the binding assays. Data represent mean values ± SD of at least four independent experiments with two different preparations of each protein (asterisks indicate the statistical significance for the comparisons between binding data at increasing NaCl concentrations with 0.1 M NaCl within each recombinant protein: *, $p < 0.05$; **, $p < 0.01$; hashes correspond to comparisons between binding data of the different mutants with WT-hA2 at 0.1 M NaCl: ##, $p < 0.01$)

Table 1
Binding of WT-hA2 and Δ14-hA2 to phosphatidylcholine (PC) and phosphatidylserine (PS) large unilamellar vesicles (LUVs).

LUVs composition	[Ca^{2+}] (μM)	Bound WT-hA2 (%)	Bound Δ14-hA2 (%)
PC	0 (1 mM EGTA)	7 ± 3	Not detected
	100	5 ± 4	2 ± 1
PS	0 (1 mM EGTA)	47 ± 4	27 ± 2
	0.5	79 ± 9	68 ± 3
	30	91 ± 3	90 ± 3
	100	100	96 ± 4

Data represent mean values ± SD corresponding to 3–4 independent experiments.

of this annexin to 1-palmitoyl-2-oleyl-sn-glycero-3-phospho-L-serine (POPS) lipids. Among them, they describe that $Lys^{49/81/88}$ and Lys^{281} are in full contact with model POPS lipids (and Lys^{279} and Lys^{286} also when phosphatidylinositol-(4,5)-bisphosphate is considered). Interestingly, we have shown that mutation of Lys^{49} and Lys^{281} to alanine residues (in addition to Lys^{206}) induces a highly significant reduction in calcium-independent binding to natural PS vesicles, in good accordance with the theoretical model proposed *in silico* [43].

As mentioned above, the calcium-independent binding to PS vesicles of Δ14-hA2 is also reduced compared to WT-hA2, but this decrease is not as large as that observed with TK-hA2, as the truncated protein can still establish electrostatic bridges with the negatively charged PS headgroups. In any case, these bridges are broken when NaCl concentration is increased, confirming the relevance of these Lys residues in the interaction.

When PS binding is studied with 100 μM $CaCl_2$, all recombinant proteins showed almost complete interaction, surely involving the canonical type II calcium and membrane binding sites. The calcium dependent interaction of WT-hA2 is quite insensitive to an increase in NaCl concentration, as occurs with the mutant forms at least up to 0.3 M NaCl.

3.4. Induction of vesicle aggregation

One of the main functions of annexin A2 is its involvement in intracellular vesicle trafficking and interaction of vesicles with membranes, as well as plasma membrane repair. Annexin A2 acts as a bridge between membranes as occurs with other annexins under specific conditions. It has been reported that annexin A2 may induce this process both in a calcium-dependent and independent manner, although the latter have been mainly reported at acidic pH values, as also described for annexin A5 and B12, and can involve both monomeric and heterotetrameric annexin A2 [8,13,14,44–46]. Several studies have been directed towards the elucidation of the mechanism by which monomeric annexin A2 induces membrane bridging under physiological conditions, as in membrane exocytosis [47] or endosomal transport [48], but still much is unclear. We have analyzed the induction of aggregation by monomeric annexin A2 in a model system consisting of PS LUVs to gain further information on the mechanisms by which this process may take place *in vivo*.

Wild-type annexin A2 induces PS vesicle aggregation in the presence of 100 μM calcium and 0.1 M NaCl even at low protein concentration (Fig. 5, black circles). Both apparent initial velocity (v_0 app.) and final ΔA_{320} show a sigmoidal pattern with protein concentration that could correspond to the induction of this process through different mechanisms at high or low protein concentration. No decrease in apparent v_0 is detected at high protein concentrations, strongly suggesting that, at least under these conditions, vesicle aggregation involves protein dimer formation. TM-hA2-induced vesicle aggregation (Fig. 5, empty squares) presents higher apparent v_0 and final ΔA_{320} values than WT-hA2, mainly at low protein concentration (p-values < 0.01). Enhanced aggregation (apparent v_0 and ΔA_{320}) is also achieved when the amphipathic α-helix is deleted (Δ14-hA2; Fig. 5, black triangles; p-values < 0.01). On the contrary, replacement of the three protruding Lys residues by Ala (TK-hA2; Fig. 5, empty diamonds) induces a strong decrease in the kinetics of aggregation ($p < 0.01$), although not in the final ΔA_{320} values, that are quite similar to those obtained with WT-hA2. This indicates that these Lys residues accelerate binding of annexin A2 to vesicles in the presence of calcium, but are not essential for calcium-dependent aggregation.

A moderate increase in ionic strength (0.3 M NaCl) induces only a slight increase in the aggregation kinetics but a highly significant increase in the final absorption values ($p < 0.01$). The increased aggregation ability at higher NaCl concentration suggests that non-electrostatic attraction forces are involved, probably through the formation of protein dimers (in accordance with data from kinetics at high protein concentration). But these dimers must be different from the "antiparallel" lateral ones described by Rosengarth and Luecke [31] as the mutant in which these salt bridges are blocked is the one with stronger aggregation ability. Moreover, the increase in NaCl concentration may disrupt the reported lateral salt bridges, favoring the formation of more aggregation-prone dimers as also suggested by Ecsédi et al. [35]. The removal of the N-terminal α-helix also enhances aggregation; in this case, one could speculate that this removal may facilitate the establishment of dimers through the concave regions of opposing annexin molecules on different vesicles. This result is in apparent contradiction with Zibouche et al. [14], which reported that annexin A2 lacking the N-terminal domain maintained the aggregation ability but far worse than wild-type. However, one has to take into account that they used a truncated annexin without the first 30 residues, not only the amphipathic N-terminal α-helix (first 14 residues).

Aggregation can also take place in the absence of calcium, but it is only detected for WT-hA2 and TM-hA2 proteins (Fig. 5a, right panels). However, both proteins present lower apparent v_0 and ΔA_{320} values compared to calcium-dependent aggregation (p-values < 0.01). Under these conditions, binding to PS vesicles was below 50%, which could justify the impaired aggregation. Interestingly, TM-hA2 shows much higher apparent v_0 values than WT-hA2 ($p < 0.01$) whereas differences where not so large considering final ΔA_{320} ($p < 0.05$). In the absence of calcium, binding to PS vesicles mainly depends on the positively charged residues in the convex side of the annexin molecule and, to a lesser extent, on potential interactions through the N-terminal α-helix. In fact, when NaCl concentration is increased, aggregation is strongly impaired (Fig. 5b) due to the weakening of the electrostatic annexin-PS interactions and consequent decrease in binding (Fig. 4).

3.5. Annexin A2 crosslinking in the absence and presence of PS LUVs

In order to check whether dimers were formed upon annexin-induced vesicle aggregation, we carried out crosslinking experiments using BS^3 (*bis*[sulfosuccinimidyl]suberate) in the absence of PS vesicles as well as with PS-bound annexin (Fig. 6). Crosslinking of annexin A2 variants in the absence of vesicles (Fig. 6; "No PS" lanes) and in the presence or absence of calcium allows the detection of protein dimers in all cases with the exception of the annexin mutant lacking the N-terminal α-helix (Δ14-hA2). An increase in ionic strength does not significantly alter dimer formation, but this dimerization is more evident in TM-hA2 in which the lateral "antiparallel" dimers reported by Rosengarth and Luecke [31] are not possible. As removal of the N-terminal α-helix completely disrupts dimer crosslinking, the detected dimers are probably dependent upon interactions of this helix with its counterpart in other annexin monomer or with a different region of the opposing molecule. Moreover, "upside-down" lateral dimers are not detected under these experimental conditions, as they are not present in crosslinking experiments in Δ14-hA2 in which these lateral interactions are theoretically possible.

High molecular weight aggregates are observed in the absence of PS, mainly in the TM-hA2 mutant. These aggregates do not correspond

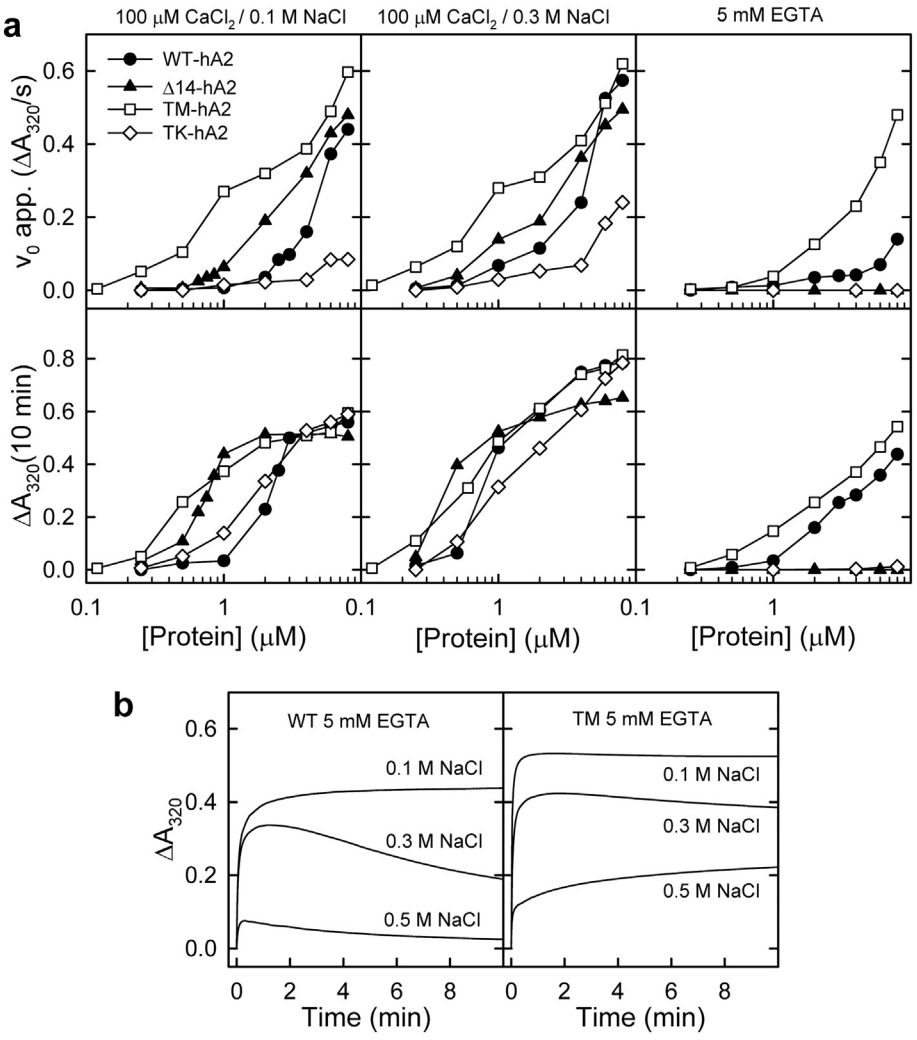

Fig. 5. Annexin-induced PS vesicle aggregation. **(a)** Aggregation of 100 nm unilamellar PS vesicles was studied as a function of protein concentration in the absence (5 mM EGTA) or presence of 100 μM $CaCl_2$. Aggregation was initiated by addition of PS vesicles to the different protein solutions at the indicated concentration in 10 mM Hepes, pH 7.8, and different NaCl concentrations. Aggregation was followed by continuously monitoring absorbance at 320 nm in a thermostatized cuvette at 25 °C. Aggregation experiments were carried out with 2 different preparations of each recombinant protein and were repeated at least twice. Data represent mean values; SD was always around or below 10% (not shown). **(b)** Aggregation curves induced by 8 μM WT-hA2 and TM-hA2 in the presence of EGTA and three different NaCl concentrations (representative curves are shown).

to poorly folded protein as all experiments were carried out with freshly prepared protein batches whose correct folding was checked by spectroscopical methods. These larger aggregates do not contribute to vesicle aggregation, as they are not present when crosslinking is carried out after the interaction with PS vesicles at physiological ionic strength (0.1 M NaCl), even in the TM-hA2 mutant, although they are again detected at higher NaCl concentration (Fig. 6).

Crosslinking experiments in the presence of PS-vesicles were carried out at a high PS to protein molar ratio to avoid potential dimerization between annexin molecules on the same vesicle. Only PS-bound annexin was analyzed after sedimentation of the different preparations. Of course, when binding was almost null (*i.e.* in the absence of calcium in TK-hA2) not even the monomers could be observed.

Crosslinking in the presence of PS-vesicles and 100 μM Ca^{2+} reveals the presence of dimers in all the constructs analyzed, including Δ14-hA2. Interestingly, TM-hA2 shows the highest dimerization degree confirming that the dimers responsible for the calcium-induced PS vesicle aggregation are not those arising from the "antiparallel" lateral interactions but rather different ones formed by non-ionic interactions between the convex surfaces of annexin molecules. Dimers are also observed in the N-terminal truncated mutant that, in addition, induces aggregation under physiological conditions even better than wild-type annexin A2. Thus, the amphipathic α-helix seems not to be involved in the formation of dimers that promote membrane aggregation. Increasing ionic strength up to 0.3 M NaCl induces a slight increase in dimer detection except in TK-hA2 (in which binding also decreases), decreasing at 0.5 M NaCl in parallel with the reduced binding.

In the absence of calcium, binding of annexin A2 variants to PS vesicles is strongly impaired (around 50% bound protein for WT-hA2 and TM-hA2, 27% for Δ14-hA2, and 12.5% for TK-A2h), but WT-hA2 and TM-hA2 are still able to induce vesicle aggregation (no aggregation is observed for Δ14-hA2 and TK-hA2). Crosslinking reveals no dimers in WT-hA2, but they are still detectable in TM-hA2. Thus, it is highly probable that annexin A2 aggregation in the absence of calcium is induced by a single molecule interacting with one vesicle through the protruding lysine residues and with the other *via* the N-terminal amphipathic α-helix. A similar mechanism has been proposed for annexin A1 [49–51]. This would be in agreement with cryo-electron microscopy studies that observed membrane junctions induced by monomeric annexin A2 [13]. These studies were carried out in the absence of calcium but these junctions were induced at non-physiological acidic pH values around 4, whereas we have been able to observe this monomeric aggregation process at neutral pH.

Finally, our results point out that the described lateral "antiparallel" dimerization described for WT-hA2 (and potentially present in Δ14-hA2 and TK-hA2) does not facilitate membrane aggregation. On the contrary, it seems to act as a regulatory mechanism that dampens this process as the TM-mutant (that lacks these interactions) has a greater ability to form dimers and aggregate vesicles (Figs. 5 & 6). In any case, this lateral dimerization may have a different role in inducing multimeric states involved in the complex functions of annexin A2.

Are dimers in the absence of phospholipid membranes identical to those detected after the interaction with membranes? Our results suggest that they are different, as the removal of the amphipathic α-helix in

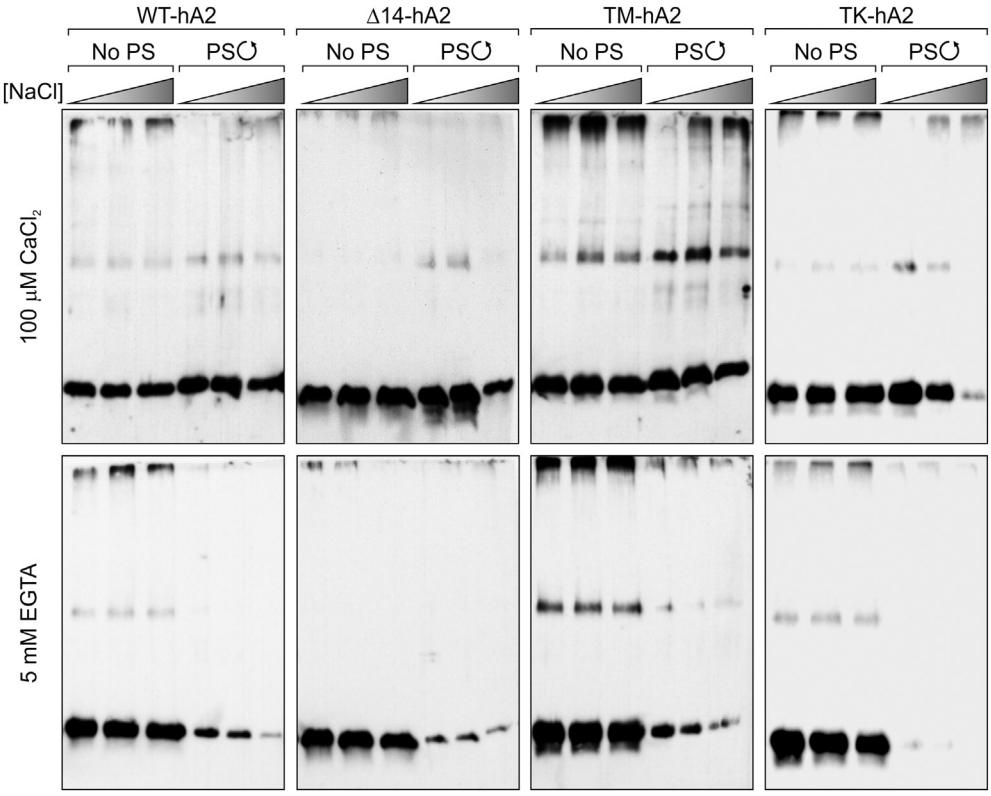

Fig. 6. Cross-linking of annexin A2 variants bound to PS unilamellar vesicles.
Crosslinking of recombinant proteins was carried out at 1000/1 phospholipid to protein molar ratio in the absence (5 mM EGTA) or presence of 100 μM Ca^{2+} and at three different NaCl concentrations (0.1, 0.3 and 0.5 M) using BS^3; after stopping the crosslinking reaction, samples were centrifuged and the vesicle-bound proteins were analyzed by Western blot (PS lanes). Controls in the absence of PS vesicles were also crosslinked ("No PS" lanes); in these cases, crosslinking was evaluated directly in aliquots without centrifugation. Cross-linking experiments were carried out at least twice with 2 different preparations of recombinant proteins; gels correspond to representative experiments.

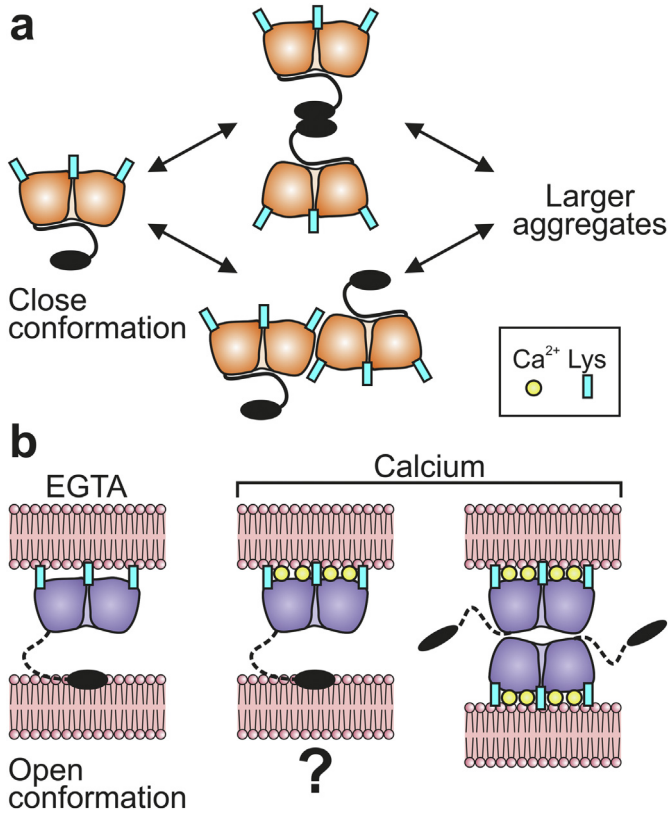

Fig. 7. Proposed models for annexin A2-induced vesicle aggregation.
(a) Possible protein oligomerization states of the closed conformation of annexin A2 in solution in the absence of membranes. **(b)** Scheme for the different possible mechanisms of vesicle aggregation induced by the open conformation of annexin A2 in the absence of calcium (EGTA) and in the presence of intracellular or extracellular calcium concentrations.

the absence of vesicles entails the disappearance of crosslinked dimers. On the other hand, dimers are again observed in Δ14-hA2 in the presence of vesicles and calcium, conditions that induce vesicle aggregation. Several authors have proposed that annexin A2 adopts different conformations in solution (closed conformation) and after binding to membranes (open conformation), in contrast to annexin A1, where calcium binding is sufficient to induce the open conformation [35,52]. Thus, dimers formed in the absence of membranes require an intact N-terminus in the closed conformation, where this region interacts with the concave surface of the protein core (Fig. 7a). Dimerization under these conditions probably requires the interaction between the N-terminal amphipathic α-helices from opposing annexin molecules. In addition, lateral "antiparallel" interactions may take place (although we have not been able to observe them after BS^3 crosslinking) as well as larger aggregates (Fig. 7a). When annexin A2 interacts with membranes, a conformational change towards an "open" conformation takes place. As suggested by Ecsédi et al. [35], the N-terminal domain under this conformation has a greater mobility and would allow the interaction between the concave surfaces of two annexin molecules in a similar pattern as occurs after phosphorylation of serine residue 26 (Fig. 7b). The existence of lateral dimers probably delays or impairs this conformational change, as vesicle aggregation triggered by the mutant lacking the lateral interactions shows a higher apparent initial velocity than wild-type annexin A2. In addition, the removal of the first 14 residues probably facilitates the acquisition of the open conformation taking into account that the Δ14-hA2 mutant induces vesicle aggregation at protein concentrations much lower than WT-hA2 and with higher apparent v_0 values.

4. Conclusions

Although many studies are centered on the physiological and pathological role of annexin A2 heterotetramer with S100A10 (p11), monomeric annexin A2 plays also important roles within different types of cells, being mainly involved in intracellular vesicle traffic such as

exocytosis [47] or in endosomal transport, aggregation and fusion [48]. Here we have designed mutant variants of human annexin A2 to increase the knowledge on the molecular mechanisms involved in annexin A2-mediated vesicle aggregation under experimental conditions resembling different cellular microenvironments.

Annexin A2 in the absence of PS vesicles adopts a close conformation where the N-terminus strongly interacts with the concave surface of the molecule [35,52]. Under these conditions, annexin A2 must present an equilibrium between monomers and dimers (formed by the interaction between N-terminal α-helices or through the formation of the so-called "antiparallel" dimers), probably together with higher molecular aggregates (Fig. 7a). Upon calcium-dependent membrane binding, a conformational change takes place towards an open conformation where the N-terminus presents higher mobility and may allow the interaction between the concave surfaces of two annexin A2 molecules leading to vesicle aggregation (Fig. 7b, right). We propose that the existence of "antiparallel" dimers could act as a regulatory mechanism to attenuate annexin A2-mediated membrane aggregation. In any case, monomeric aggregation cannot be completely discarded, mainly at low protein concentration.

In the absence of calcium, aggregation of acidic vesicles seems to depend on annexin A2 monomers acting as a bridge between two opposing membranes instead of dimers. The convex surface interacts with one of the negatively charged membranes through protruding Lys residues, and the N-terminal amphipathic α-helix with the other (Fig. 7b, left). On the other hand, calcium-dependent aggregation probably involves the formation of annexin A2 dimers through their concave uncharged surfaces without apparent significant involvement of the N-terminal α-helix (Fig. 7b, right), although it cannot be discarded that aggregation may be also triggered by annexin monomers (Fig. 7b, middle).These results would be in agreement with cryo-electron microscopy experiments carried out by Lambert et al. [13] at neutral pH in the presence of calcium using chromaffin granules as well as artificial liposomes, where they detected annexin A2 between two membranes mainly in a double protein layer and less frequently as a single one.

Transparency document

The Transparency document associated with this article can be found, in online version.

Acknowledgments

We are thankful to the staff from the Genomics and Proteomics Center from the Complutense University of Madrid for their skillful assistance.

Funding

This work was supported by the Santander-UCM grant [PR26/16-20323] to J.T., and J.C.L.-R. is recipient of an FPU fellowship from the Spanish Ministry of Education, Culture and Sports [FPU13/02393].

Appendix A. Supplementary data

Cloning, expression and purification of recombinant annexin A2 and mutants. Supplementary Figs. 1 & 2. Supplementary data to this article can be found online at doi: https://doi.org/10.1016/j.bbamcr.2018.03.010.

References

[1] V. Gerke, S.E. Moss, Annexins: from structure to function, Physiol. Rev. 82 (2002) 331–371.
[2] S.E. Moss, R.O. Morgan, The annexins, Genome Biol. 5 (2004) 219.
[3] M.A. Lizarbe, J.I. Barrasa, N. Olmo, F. Gavilanes, J. Turnay, Annexin-phospholipid interactions. Functional implications, Int. J. Mol. Sci. 14 (2013) 2652–2683.
[4] J. Turnay, E. Lecona, A. Guzmán-Aránguez, P. Pérez-Ramos, S. Fernández-Lizarbe, N. Olmo, M.A. Lizarbe, Annexins: structural characteristics of the N-terminus and influence on the overall structure of the protein, Recent Res. Dev. Biochem. 4 (2003) 79–95.
[5] V. Gerke, C.E. Creutz, S.E. Moss, Annexins: linking Ca2+ signalling to membrane dynamics, Nat. Rev. Mol. Cell. Biol. 6 (2005) 449–461.
[6] J. Ayala-Sanmartin, J.P. Henry, L.A. Pradel, Cholesterol regulates membrane binding and aggregation by annexin 2 at submicromolar Ca(2+) concentration, Biochim. Biophys. Acta 1510 (2001) 18–28.
[7] L. Liu, A.B. Fisher, U.J. Zimmerman, Lung annexin II promotes fusion of isolated lamellar bodies with liposomes, Biochim. Biophys. Acta 1259 (1995) 166–172.
[8] M. Jost, D. Zeuschner, J. Seemann, K. Weber, V. Gerke, Identification and characterization of a novel type of annexin-membrane interaction: Ca2+ is not required for the association of annexin II with early endosomes, J. Cell Sci. 110 (Pt 2) (1997) 221–228.
[9] J. Ayala-Sanmartin, P. Gouache, J.P. Henry, N-terminal domain of annexin 2 regulates Ca(2+)-dependent membrane aggregation by the core domain: a site directed mutagenesis study, Biochemistry 39 (2000) 15190–15198.
[10] N. Johnsson, G. Marriott, K. Weber, p36, the major cytoplasmic substrate of src tyrosine protein kinase, binds to its p11 regulatory subunit via a short amino-terminal amphiphatic helix, EMBO J. 7 (1988) 2435–2442.
[11] A.R. Nazmi, G. Ozorowski, M. Pejic, J.P. Whitelegge, V. Gerke, H. Luecke, N-terminal acetylation of annexin A2 is required for S100A10 binding, Biol. Chem. 393 (2012) 1141–1150.
[12] D.M. Sullivan, N.B. Wehr, M.M. Fergusson, R.L. Levine, T. Finkel, Identification of oxidant-sensitive proteins: TNF-alpha induces protein glutathiolation, Biochemistry 39 (2000) 11121–11128.
[13] O. Lambert, N. Cavusoglu, J. Gallay, M. Vincent, J.L. Rigaud, J.P. Henry, J. Ayala-Sanmartin, Novel organization and properties of annexin 2-membrane complexes, J. Biol. Chem. 279 (2004) 10872–10882.
[14] M. Zibouche, M. Vincent, F. Illien, J. Gallay, J. Ayala-Sanmartin, The N-terminal domain of annexin 2 serves as a secondary binding site during membrane bridging, J. Biol. Chem. 283 (2008) 22121–22127.
[15] L. Liu, J.Q. Tao, U.J. Zimmerman, Annexin II binds to the membrane of A549 cells in a calcium-dependent and calcium-independent manner, Cell. Signal. 9 (1997) 299–304.
[16] P. Drucker, M. Pejic, H.J. Galla, V. Gerke, Lipid segregation and membrane budding induced by the peripheral membrane binding protein annexin A2, J. Biol. Chem. 288 (2013) 24764–24776.
[17] P. Drucker, M. Pejic, D. Grill, H.J. Galla, V. Gerke, Cooperative binding of annexin A2 to cholesterol- and phosphatidylinositol-4,5-bisphosphate-containing bilayers, Biophys. J. 107 (2014) 2070–2081.
[18] S.N. Koerdt, V. Gerke, Annexin A2 is involved in Ca(2+)-dependent plasma membrane repair in primary human endothelial cells, Biochim. Biophys. Acta 1864 (2017) 1046–1053.
[19] B.M. Andersen, J. Xia, A.L. Epstein, J.R. Ohlfest, W. Chen, B.R. Blazar, C.A. Pennell, M.R. Olin, Monomeric annexin A2 is an oxygen-regulated toll-like receptor 2 ligand and adjuvant, J. Immunother. Cancer 4 (2016) 11.
[20] A.W. Woodham, A.M. Sanna, J.R. Taylor, J.G. Skeate, D.M. Da Silva, L.V. Dekker, W.M. Kast, Annexin A2 antibodies but not inhibitors of the annexin A2 heterotetramer impair productive HIV-1 infection of macrophages in vitro, Virol. J. 13 (2016) 187.
[21] T.B. McNeely, D.C. Shugars, M. Rosendahl, C. Tucker, S.P. Eisenberg, S.M. Wahl, Inhibition of human immunodeficiency virus type 1 infectivity by secretory leukocyte protease inhibitor occurs prior to viral reverse transcription, Blood 90 (1997) 1141–1149.
[22] N.A. Lokman, M.P. Ween, M.K. Oehler, C. Ricciardelli, The role of annexin A2 in tumorigenesis and cancer progression, Cancer Microenviron. 4 (2011) 199–208.
[23] J. Tsunezumi, K. Yamamoto, S. Higashi, K. Miyazaki, Matrilysin (matrix metalloprotease-7) cleaves membrane-bound annexin II and enhances binding of tissue-type plasminogen activator to cancer cell surfaces, FEBS J. 275 (2008) 4810–4823.
[24] W.S. Gilmore, S. Olwill, H. McGlynn, H.D. Alexander, Annexin A2 expression during cellular differentiation in myeloid cell lines, Biochem. Soc. Trans. 32 (2004) 1122–1123.
[25] J.K. Hitchcock, A.A. Katz, G. Schafer, Dynamic reciprocity: the role of annexin A2 in tissue integrity, J. Cell Commun. Signal 8 (2014) 125–133.
[26] S. Fernández-Lizarbe, E. Lecona, A. Santiago-Gómez, N. Olmo, M.A. Lizarbe, J. Turnay, Structural and lipid-binding characterization of human annexin A13a reveals strong differences with its long A13b isoform, Biol. Chem. 398 (2017) 359–371.
[27] E. Lecona, J. Turnay, N. Olmo, A. Guzmán-Aránguez, R.O. Morgan, M.P. Fernández, M.A. Lizarbe, Structural and functional characterization of recombinant mouse annexin A11: influence of calcium binding, Biochem. J. 373 (2003) 437–449.
[28] J. Turnay, E. Lecona, S. Fernández-Lizarbe, A. Guzmán-Aránguez, M.P. Fernández, N. Olmo, M.A. Lizarbe, Structure-function relationship in annexin A13, the founder member of the vertebrate family of annexins, Biochem. J. 389 (2005) 899–911.
[29] J. Turnay, N. Olmo, M. Gasset, I. Iloro, J.L. Arrondo, M.A. Lizarbe, Calcium-dependent conformational rearrangements and protein stability in chicken annexin A5, Biophys. J. 83 (2002) 2280–2291.
[30] A. Perczel, K. Park, G.D. Fasman, Analysis of the circular dichroism spectrum of proteins using the convex constraint algorithm: a practical guide, Anal. Biochem. 203 (1992) 83–93.
[31] A. Rosengarth, H. Luecke, Annexin A2. Does it induce membrane aggregation by a new multimeric state of the protein? Annexins 1 (2004) e34–e41.
[32] A.J. Avila-Sakar, R.H. Kretsinger, C.E. Creutz, Membrane-bound 3D structures

reveal the intrinsic flexibility of annexin VI, J. Struct. Biol. 130 (2000) 54–62.
[33] R. Gautier, D. Douguet, B. Antonny, G. Drin, HELIQUEST: a web server to screen sequences with specific alpha-helical properties, Bioinformatics 24 (2008) 2101–2102.
[34] S. Rety, J. Sopkova, M. Renouard, D. Osterloh, V. Gerke, S. Tabaries, F. Russo-Marie, A. Lewit-Bentley, The crystal structure of a complex of p11 with the annexin II N-terminal peptide, Nat. Struct. Biol. 6 (1999) 89–95.
[35] P. Ecsédi, B. Kiss, G. Gógl, L. Radnai, L. Buday, K. Koprivanacz, K. Liliom, I. Leveles, B. Vértessy, N. Jeszenői, C. Hetényi, G. Schlosser, G. Katona, L. Nyitray, Regulation of the equilibrium between closed and open conformations of annexin A2 by N-terminal phosphorylation and S100A4-binding, Structure 25 (2017) 1195–1207 (e1195).
[36] Y.H. Hong, H.S. Won, H.C. Ahn, B.J. Lee, Structural elucidation of the protein- and membrane-binding properties of the N-terminal tail domain of human annexin II, J. Biochem. 134 (2003) 427–432.
[37] J. Ayala-Sanmartin, M. Vincent, J. Sopkova, J. Gallay, Modulation by Ca(2+) and by membrane binding of the dynamics of domain III of annexin 2 (p36) and the annexin 2-p11 complex (p90): implications for their biochemical properties, Biochemistry 39 (2000) 15179–15189.
[38] A.M. Hofer, Another dimension to calcium signaling: a look at extracellular calcium, J. Cell Sci. 118 (2005) 855–862.
[39] J. Leipziger, R. Nitschke, R. Greger, Regulation of the intracellular calcium concentration in epithelial cells, Kidney Blood Press. Res. 19 (1996) 148–150.
[40] P. Pizzo, V. Lissandron, P. Capitanio, T. Pozzan, Ca(2+) signalling in the Golgi apparatus, Cell Calcium 50 (2011) 184–192.
[41] A. Burger, R. Berendes, S. Liemann, J. Benz, A. Hofmann, P. Gottig, R. Huber, V. Gerke, C. Thiel, J. Romisch, K. Weber, The crystal structure and ion channel activity of human Annexin II, a peripheral membrane protein, J. Mol. Biol. 257 (1996) 839–847.
[42] J.R. Lakowicz, Quenching of fluorescence, in: J.R. Lakowicz (Ed.), Principles of Fluorescence Spectroscopy, Springer, Place Published, 2006, pp. 278–320.
[43] D. Hakobyan, V. Gerke, A. Heuer, Modeling of annexin A2-membrane interactions by molecular dynamics simulations, PLoS One 12 (2017) e0185440.
[44] J.M. Isas, J.P. Cartailler, Y. Sokolov, D.R. Patel, R. Langen, H. Luecke, J.E. Hall, H.T. Haigler, Annexins V and XII insert into bilayers at mildly acidic pH and form ion channels, Biochemistry 39 (2000) 3015–3022.
[45] G. Kohler, U. Hering, O. Zschornig, K. Arnold, Annexin V interaction with phosphatidylserine-containing vesicles at low and neutral pH, Biochemistry 36 (1997) 8189–8194.
[46] S.P. Lauritzen, T.L. Boye, J. Nylandsted, Annexins are instrumental for efficient plasma membrane repair in cancer cells, Semin. Cell Dev. Biol. 45 (2015) 32–38.
[47] S. Chasserot-Golaz, N. Vitale, I. Sagot, B. Delouche, S. Dirrig, L.A. Pradel, J.P. Henry, D. Aunis, M.F. Bader, Annexin II in exocytosis: catecholamine secretion requires the translocation of p36 to the subplasmalemmal region in chromaffin cells, J. Cell Biol. 133 (1996) 1217–1236.
[48] E. Morel, J. Gruenberg, The p11/S100A10 light chain of annexin A2 is dispensable for annexin A2 association to endosomes and functions in endosomal transport, PLoS One 2 (2007) e1118.
[49] M.P. Donohue, L.J. Bartolotti, Y. Li, The N-terminal of annexin A1 as a secondary membrane binding site: a molecular dynamics study, Proteins 82 (2014) 2936–2942.
[50] A. Rosengarth, V. Gerke, H. Luecke, X-ray structure of full-length annexin 1 and implications for membrane aggregation, J. Mol. Biol. 306 (2001) 489–498.
[51] A. Rosengarth, H. Luecke, A calcium-driven conformational switch of the N-terminal and core domains of annexin A1, J. Mol. Biol. 326 (2003) 1317–1325.
[52] C. Bellagamba, I. Hubaishy, J.D. Bjorge, S.L. Fitzpatrick, D.J. Fujita, D.M. Waisman, Tyrosine phosphorylation of annexin II tetramer is stimulated by membrane binding, J. Biol. Chem. 272 (1997) 3195–3199.
[53] R. Koradi, M. Billeter, K. Wuthrich, MOLMOL: a program for display and analysis of macromolecular structures, J. Mol. Graph. 14 (1996) 51–55 (29-32).